



Imaging of lung pathology in COVID-19 (literature review and own data)

Igor E. Tyurin , Anastasia D. Strutynskaya

Russian Federal Academy of Continued Medical Education, Healthcare Ministry of Russia: ul. Barrikadnaya 2/1, build. 1, Moscow, 123995, Russia

Abstract

Novel coronavirus infection is predominantly manifests as lung tissue damage. Imaging methods, particularly, chest X-Ray and computed tomography, are of great importance for detecting pulmonary changes and differentiate them with other diseases (mainly other viral pneumonias). In the early disease stages the disease presents on CT with ground glass opacities, consolidations, crazy paving symptom. With time course, they can gradually decrease, evolve into organizing pneumonia or stay stable and even increase in volume with the spread of consolidation and formation of several signs of organizing pneumonia. Although radiological methods show high sensitivity in the detection of pulmonary changes, their specificity and prognostic ability are not so good today. Novel coronavirus infection can be complicated with pulmonary embolism, development thrombosis *in situ* in pulmonary small vessels, acute heart failure and subsequent development of cardiogenic pulmonary edema, bacterial superinfection, exacerbation or worsening of chronic lung disease and several iatrogenic issues (pneumothorax, pneumomediastinum, hematomas).

Key words: novel coronavirus disease, computed tomography, diffuse alveolar damage, organizing pneumonia, complication.

Conflict of interests. The authors declare the absence of conflict of interests.

For citation: Tyurin I.E., Strutynskaya A.D. Imaging of lung pathology in COVID-19 (literature review and own data). *Pul'monologiya*. 2020; 30 (5): 658–670 (in Russian). DOI: 10.18093/0869-0189-2020-30-5-658-670

Визуализация изменений в легких при коронавирусной инфекции (обзор литературы и собственные данные)

И.Е.Тюрин , А.Д.Струтынская

Федеральное государственное бюджетное образовательное учреждение дополнительного профессионального образования «Российская медицинская академия непрерывного профессионального образования» Министерства здравоохранения Российской Федерации: 125993, Россия, Москва, ул. Баррикадная, 2 / 1, стр. 1

Резюме

Одним из главных проявлений новой коронавирусной инфекции (КВИ) является поражение легочной ткани, при этом для выявления изменений в легких и их дифференциальной диагностики с другими заболеваниями (преимущественно иными вирусными пневмониями) большую роль играют методы визуализации, в первую очередь – обзорная рентгенография и компьютерная томография. В начале заболевания в большинстве случаев определяется уплотнение легочной ткани по типу «матового стекла» или консолидации, симптом «бульжной мостовой». Данные изменения при динамическом исследовании могут уменьшиться в объеме с постепенным восстановлением воздушности легочной паренхимы или нарастанием консолидации и формированием типичной картины организуемой пневмонии. Они могут сохраняться и даже увеличиваться с нарастанием консолидации, появлением типичной картины или отдельных признаков организуемой пневмонии. Однако при высокой чувствительности методов лучевой диагностики на сегодняшний день их специфичность и прогностическая способность остаются не столь высокими. Осложнениями КВИ являются тромбоэмболия легочной артерии, развитие тромбозов легочных сосудов *in situ*, острая сердечная недостаточность с развитием кардиогенного отека легких, бактериальная суперинфекция, обострение или ухудшение хронического заболевания легких и последствия проводимой терапии (пневмоторакс, пневмомедиастинум, гематомы).

Ключевые слова: новая коронавирусная инфекция, компьютерная томография, диффузное альвеолярное повреждение, организуемая пневмония, осложнение.

Конфликт интересов. Авторы заявляют об отсутствии конфликта интересов.

Для цитирования: Тюрин И.Е., Струтынская А.Д. Визуализация изменений в легких при коронавирусной инфекции (обзор литературы и собственные данные). *Пульмонология*. 2020; 30 (5): 658–670. DOI: 10.18093/0869-0189-2020-30-5-658-670

The world has been affected by the novel coronavirus infection (COVID-19) since December 2019, when the coronavirus SARS-CoV-2 was first isolated from patients in the Chinese city of Wuhan. Since then, the number of new cases worldwide has been increasing steadily. Lung damage is the main manifestation of this infection, which is seen almost in all cases and defined as “viral pneumonia”. The need is clear for timely and accurate assessment

of abnormal chest findings, appropriate assessment of these changes over time, and evaluation of the prognostic value of the main radiographic signs of organ damage. Imaging techniques are particularly important for detecting pulmonary changes caused by SARS-CoV-2, differentiating them from those caused by other disorders, assessing the severity of abnormal findings and changes in them over time, and evaluating the efficacy of treatment.

Imaging techniques

Imaging techniques used to detect pulmonary abnormalities in patients with COVID-19 include plain chest X-ray and chest computed tomography (CT), and, in some cases, pulmonary and pleural ultrasound. Magnetic resonance imaging and radionuclide imaging have no diagnostic significance for acute respiratory infections and are not used to detect lung damage in COVID-19.

During the first days of the disease, the sensitivity of routine X-ray for early changes in the lungs (ground-glass opacities) is relatively low, and this technique cannot be used to exclude COVID-19 during this period [1, 2]. At later stages, however, the diagnostic value of X-ray significantly increases as the disease becomes more generalised and pulmonary consolidation progresses. This method reliably detects severe viral lung disease and pulmonary oedema of various etiologies. Portable chest X-ray obtained using mobile units is the main diagnostic imaging modality for chest abnormalities in resuscitation and intensive care units. This type of X-ray is recommended in most clinical guidelines as the most readily available and epidemiologically safe imaging technique.

Computed tomography is the most sensitive tool to detect radiographic signs of COVID-19. CT is feasible for initial chest evaluation in patients with severe, progressive disease and patients with clinical signs of acute viral respiratory infections and evident risk factors for a severe course of infection. Also CT is necessary for differential diagnosis of the findings revealed and, in some cases, for follow-up evaluation. The main drawback of CT is its low specificity, which rarely exceeds 60%, as it reveals multiple unequivocal lesions, such as small ground-glass opacities or reticular lesions. The specificity of CT also depends on the prevalence of infection in a particular area [1, 3–6]. The higher percentage of people are infected, the more specific CT becomes, and vice versa. The specificity of CT scanning is also highly dependent on the probability of the disease in an individual patient. The lower the clinical probability is, the less specific CT findings are.

Due to their low specificity, none of imaging modalities is recommended as a screening tool to detect respiratory problems in asymptomatic persons and patients with mild disease. In addition, imaging techniques cannot identify the etiology of the disease and, therefore, cannot replace routine laboratory tests.

Ultrasonography is an adjunctive imaging tool, which does not replace or exclude CT scanning and X-ray. When its technique is well respected and the examination is performed by a qualified specialist, ultrasonography is highly sensitive for the detection of subpleural interstitial changes and consolidations in lung tissue, pleural effusion, and pneumothorax [7–9].

The role of ultrasound in assessing pulmonary abnormalities in COVID-19 patients is controversial. Despite their high sensitivity, ultrasound data are not helpful in assessing the actual extent of lung injury. Ultrasound findings do not always correlate with X-ray and CT data. Finally, ultrasonography is not a standard diagnostic tool to diagnose pneumonia and not included in clinical guidelines for the diagnosis and treatment of communi-

ty-acquired pneumonia. Therefore, its diagnostic value depends largely on the experience and qualifications of physicians in a particular facility.

Comparison of radiographic morphological features

It has been established that SARS-CoV-2 binds to angiotensin-converting enzyme 2 (ACE2), a membrane receptor expressed mainly on the surface of nasal epithelial cells, lower airway cells, particularly type II alveolar cells, as well as cells in the upper third of the oesophagus, enterocytes of the colon, cholangiocytes, cardiomyocytes, and epithelial cells in the proximal renal tubules and the bladder. Therefore, the airway epithelium serves as the standard entry point for this infection; from there the virus moves to the blood and affects the most susceptible organs and tissues [11–13].

Viral exposure in the lungs usually triggers diffuse alveolar damage (DAD). This term is used to describe characteristic changes in all layers of the alveolar-capillary membrane, including its basal membrane [13–17]. DAD typically is a biphasic process, and includes exudative (oedematous) and proliferative phases.

The exudative phase develops within the first few days and manifests as inflammation in the area damaged by the virus. This is accompanied by breaches in alveolar epithelium and, in some cases, sloughing of alveolar epithelial cells from the basal membrane. Some histochemical reactions and the loss of the integrity of the alveolar-capillary barrier result in exacerbation of interstitial oedema and filling of the alveoli with a fluid rich in proteins, particularly fibrin. An important step of this process is the formation of hyaline membranes, one of the main morphological markers of DAD, in the alveolar spaces.

Partial filling of the alveoli with exudate, cellular debris, and hyaline membranes is responsible for ground-glass opacities, the earliest and the most typical sign of viral lung damage detected by various imaging modalities. As abnormal contents continues to accumulate in the alveolar spaces, images start to show consolidations, areas of completely airless lung parenchyma, which are usually surrounded by a peripheral ring of ground-glass opacity (halo sign).

Viral damage to the alveolar-capillary membrane may spread throughout the interstitial compartment and affect pulmonary capillary endothelial cells. Breakdown of capillary endothelial lining cells and those anchored to the basal membrane results in the following two consequences: damage to the capillary wall (basal membrane) and an outpouring of haemorrhagic exudate directly into the alveolar spaces and the interstitial compartment, on the one hand, and thrombosis of small pulmonary vessels [17].

Radiographically, accumulation of haemorrhagic exudate in alveoli also manifests as ground-glass opacities, which relatively rapidly develop into consolidation. Ground-glass opacity lesions often have areas of reticular abnormality seen as polygonal structures 5 to 15 mm in diameter, which are actually thickened intralobular or interlobular septa (Figure 1). This is the well-known crazy

paving sign. It is not specific for viral lung damage. It can also be seen in a number of other infections, as well as in neoplasms, interstitial disorders, pulmonary oedema of various etiologies, pulmonary haemorrhage, and in case of blood aspiration in patients with pulmonary bleeding [18–20]. Some studies showed that the crazy paving sign predicts a poor prognosis for coronavirus infection, which has been reflected in many recent guidelines [5].

On radiographic images, bleeding into the alveoli or blood accumulation in the alveolar spaces, on the one hand, and cellular debris with hyaline membranes in the alveoli, on the other, manifest identically, i.e. as ground-glass opacity and consolidation. Radiography does not provide reliable evidence to distinguish between these morphological changes. However, the prognostic value of these imaging signs and clinical features associated with them turn out to be completely different, even in patients with similar extent of lung injury. Haemorrhagic suffusion of lung tissue is often a harbinger of acute respiratory distress syndrome. Some authors believe that haemorrhagic oedema is the cause of exceptionally fast progression of pulmonary abnormalities in patients with an initially small area of lung involvement [21–24].

On a chest radiograph, thrombosis of small pulmonary vessels is seen as dilation of these vessels in areas of increased density with the ground-glass pattern, but not in consolidation areas, where vessels are not seen on a background of airless lung. This sign is most evident in the cortical lung zones within the first few days (see Figure 1).

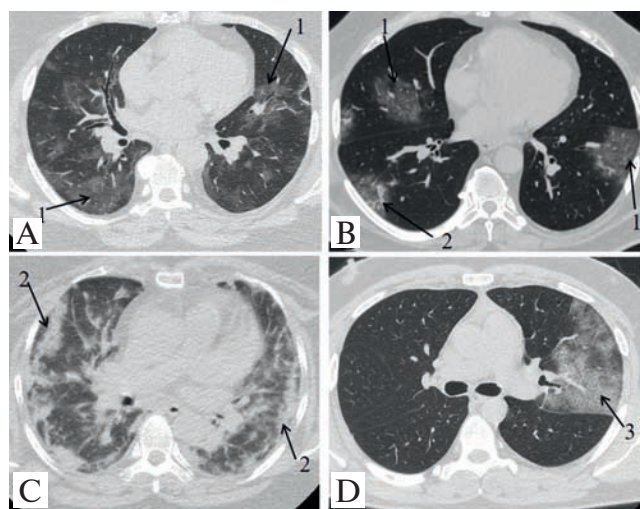


Figure 1. Variants of manifestation of COVID-19 (computed tomography on the 5–7th days of the disease): A, bilateral subpleural and peribronchovascular ground glass foci (1) of irregular shape; B, bilateral ground glass foci (1) with small consolidation areas (2) located subpleurally and in the central areas of lungs; C, bilateral subpleural confluent round areas of consolidation (2); D, crazy paving sign (3) in the upper left lobe

Рис. 1. Варианты манифестации COVID-19 (компьютерная томография выполнена на 5–7-е сутки от начала заболевания): А – билатеральные субплевральные и перибронховаскулярные участки «матового стекла» (1) неправильной формы; В – билатеральные участки «матового стекла» (1) в сочетании с небольшими участками консолидации (2) округлой формы, расположенные субплеврально и в центральных отделах легких; С – билатеральные сливные участки консолидации (2), расположенные преимущественно субплеврально; D – симптом «булыжной мостовой» (3) в верхней доле левого легкого

The proliferative phase of DAD becomes more prominent over the second or third week of the disease. This period is marked by dissolution of hyaline membranes, formation of immature connective tissue in the alveolar spaces and respiratory bronchioles, hyperplasia of type II alveolar cells, and migration of fibroblasts, monocytes, and macrophages to damaged alveoli. Morphologically, this process is usually viewed as an organising pneumonia. In this phase, the course of the disease depends on the volume and depth of the affected parenchyma and the integrity of the alveolar-capillary membrane [18, 20]. When all components are involved and the basal membrane is degraded, which is typically seen in COVID-19, the convalescence phase is almost unavoidably manifests as organizing pneumonia (OP). When lung tissue is not so deeply affected, complete restoration of lung parenchyma is possible without elements of OP, similar to how it happens in common bacterial pneumonia [18, 20].

The radiographic findings of OP are well established and frequently described in literature (Figure 2). These often include signs of cryptogenic OP and OP of known etiologies, such as drug exposure, viral and other infections, radiation damage, and systemic connective tissue diseases [24–27]. A typical imaging sign of this disorder is the presence of multiple patchy ground-glass density lesions combined with consolidations. They can be located in subpleural, perilobular, or peribronchial regions. An obligatory feature is the air bronchogram sign, i.e. the phenomenon of air-filled bronchi being made visible by

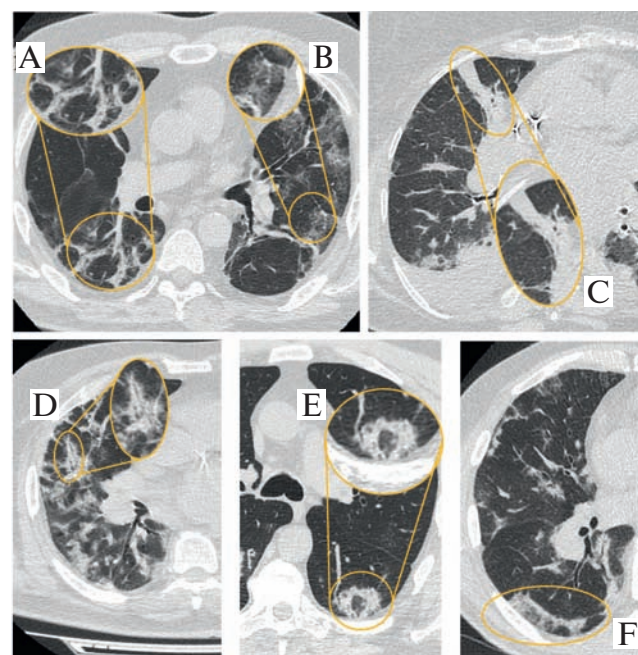


Figure 2. Common computed tomography signs of organizing pneumonia: A, perilobular reticular pattern; B, reticulation; C, linear consolidation; D, peribronchovascular consolidation; E, atoll sign (reversed halo sign); F, fibrous band parallel to pleura

Рис. 2. Типичные компьютерно-томографические признаки организуемой пневмонии: А – перилобулярный ретикулярный паттерн; В – ретикулярный паттерн; С – линейная консолидация; D – перибронхиальный участок консолидации; E – симптом обратного ободка («симптом атолла»); F – фиброзный тяж, параллельный плевре

the opacification of surrounding tissue. However, the key, but not disease-specific, sign of OP is the reversed halo sign, characterised by a central ground-glass opacity surrounded by a ring of consolidation. It was earlier often referred to as the atoll sign due to its appearance similar to that natural structure. It is typical to visualize on plain radiographs a gradual relocation of opacities from the visceral pleura towards deeper zones of lung parenchyma and apparent lung hyperinflation along the thoracic wall [26]. In some cases, it gives a false impression of emerging cavitating lesions or emphysematous bullae in the cortical regions.

So far, no evident temporal distinction has been determined between the DAD phases in the coronavirus infection. In many cases, it is just possible to note the predominance of a particular pathological process at a certain time point. Another specific feature of this infection is a paradoxical prolongation of any phase up to several weeks. Therefore, accurate evaluation of radiographic findings is very meaningful in practice, including in prognosis assessment.

In some patients SARS-CoV-2 specifically affects the immune system, causing uncontrolled and, in most cases, irreversible autoinflammatory response. This is accompanied by a rapid progression of the exudative phase of lung injury [22, 28, 29]. An X-ray examination reveals a rapid increase in lung involvement coupled with a fast progression of consolidation toward subtotal lung involvement (Figure 3) [30]. Pleural effusion is a frequent accompanying sign. Clinically, these findings are associated with acute respiratory distress syndrome (ARDS).

Prevalence of the primary radiographic signs

The radiographic signs of lung damage in COVID-19 patients have been described in many studies published in recent months, including large systematic analyses [31, 32]. Evaluation of CT data of more than 1,000 patients with verified coronavirus infection revealed the following most typical changes: ground-glass opacities (88.0%), bilateral lung involvement (87.5%), peripheral distribution in lung parenchyma (76.0%), and multilobar involvement (damage to more than one lobe) (78.8%) (Table 1). Isolated ground-glass opacities or accompanied by consolidation were the most common feature of the disease. Other, less common features, included intralobular and interlobular septal thickening, bronchiectasis, and pleural thickening. Pleural effusion, pericardial effusion, lymphadenopathy, cavitation, the halo sign, and pneumothorax were significantly less common (Table 2).

Changes in the radiographic signs over time

In their study *Y.H.Jin et al.* [34] described CT findings observed during five stages of COVID-19 infection, which they defined as ultra-early stage, early stage, progression stage, consolidation stage, and dissipation stage: In the ultra-early stage, one or two weeks after contraction, when patients usually had no clinical manifestations, CT

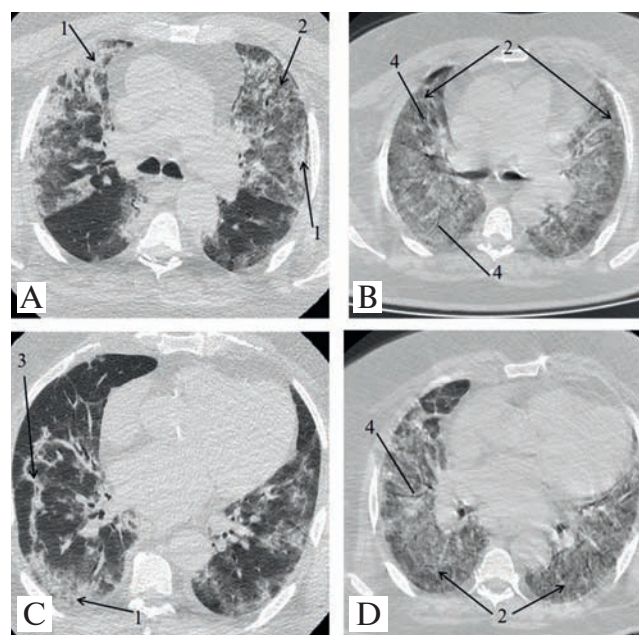


Figure 3. Patient S. 67 years old. Severe COVID-19 complicated by ARDS on the 20th day of the disease. Computed tomography, axial slices, 14th (A, B) and 20th (C, D) days of the disease; A, B, bilateral consolidation (1) and ground glass (2) foci and linear consolidation parallel to pleura (3); total lung involvement is more than 50%; C, D, total bilateral ground glass (2) spread with air bronchogram (4); damaged pulmonary area reaches 100%

Рис. 3. Пациент С., 67 лет. Тяжелое течение COVID-19 с развитием острого респираторного дистресс-синдрома на 20-е сутки заболевания. Аксиальные компьютерно-томографические срезы на: А, В – 14-е сутки заболевания; С, Д – 20-е сутки заболевания; А, В – двусторонние участки консолидации (1) и «матового стекла» (2), линейный участок консолидации вдоль плевры (3); суммарная площадь поражения легочной паренхимы > 50 %; С, Д – тотальное распространение «матового стекла» (2) с симптомом «воздушной бронхографии» (4); суммарная площадь поражения легочной паренхимы достигает 100 %

scanning showed single or multiple ground-glass opacities, and patchy consolidations or nodules surrounded by ground-glass opacities. In the early stage (early clinical manifestations, 54% in this study), CT revealed single or multiple ground-glass opacities, combined with the crazy paving pattern. In the progression stage (3 – 7 days after the onset of clinical symptoms), the disease manifested on CT as large-scale consolidation with air bronchogram inside. In the consolidation stage (the second week of clinical manifestations), CT features may include consolidations in slighter density and smaller range. About two or three weeks after the onset of symptoms, CT scanning may show patchy consolidation, linear opacities, bronchial wall thickening, and interlobular septal thickening.

E.Song et al. [35] showed that CT data reflect progression of the disease, including a higher incidence rate of consolidations. *Y.Pan et al.* [36] examined 63 patients and assessed their follow-up CT obtained 3 – 14 days after the initial CT scans. In more than 85% of patients, they found radiographic signs of disease progression, including larger areas of ground-glass opacity and consolidation and interlobular septal thickening. In some patients with lung lesions on the initial CT scans, re-examination CT showed that the lesions increased and enlarged, and some of them merged.

Table 1
Frequent symptoms and distribution of changes on computed tomography Images of patients (n = 919) with coronavirus infection [32]
Таблица 1
Частые симптомы и распределение компьютерно-томографических изменений у пациентов (n = 919) с коронавирусной инфекцией [32]

| Signs / Findings | Number of publications | Number of cases (%) | Total number of patients |
|-----------------------------------------|------------------------|---------------------|--------------------------|
| Bilateral involvement | 12 | 435 (87.5) | 497 |
| Peripheral distribution | 12 | 92 (76.0) | 121 |
| Predominantly in the posterior segments | 1 | 41 (80.4) | 51 |
| Multilobar involvement | 5 | 108 (78.8) | 137 |
| Ground-glass opacities | 22 | 346 (88.0) | 393 |
| Consolidation | 10 | 65 (31.8) | 204 |

F.Pan et al. [37] reviewed the changes in CT findings over time in 21 patients with confirmed COVID-19. In most patients, CT performed at early stages revealed more ground-glass lesions and involvement of fewer pulmonary lobes than follow-up CT scans obtained at later stages. However, when patients were re-examined some time later, their CT showed progression of reticular changes (increase in the crazy-paving pattern), involvement of more pulmonary lobes, and consolidations. On average, the CT features were most prominent on day 10 from symptom onset. After day 14 positive changes were observed in 75% of the patients and included involvement of fewer pulmonary lobes, disappearance of the crazy-paving pattern, and resolution of consolidation.

Following the initial examination, the radiographic features of viral lung damage can evolve in several ways, including the following (Table 3) [3–5, 33, 39–42]:

- Reduction in lung involvement accompanied by improvement in pulmonary aeration and dissipation of consolidations into ground-glass opacities and subsequent complete recovery of aerated lung volume. This process is reminiscent of the typical resolution stage of community-acquired pneumonia.
- Reduction in lung involvement accompanied by more prominent consolidation and appearance of a typical organising pneumonia pattern.
- Stability or even an increase in lung involvement accompanied by more prominent consolidation and appearance of a typical organising pneumonia pattern or separate signs of organising pneumonia.

The first variant is the most favourable because it indicates resolution of viral lung damage usually without any residual abnormalities. The second variant indicates a typical reparative process manifested by signs of organising pneumonia that appear in the second phase of DAD. It is a longer process, which may lead to residual pulmonary abnormalities. The long-term prognosis for patients with

Table 2
Variants of radiological manifestation of novel coronavirus infection [33]
Таблица 2
Варианты рентгенологической картины новой коронавирусной инфекции [33]

| Typical | Equivocal | Atypical |
|-------------------------------------------------------------------------------------------------------------------------------------------|-----------|----------------------------------------------------------------------------------------|
| Multiple bilateral peripheral (subpleural) ground-glass opacities: | – | Lobar consolidation |
| • including those accompanied by consolidation | | Focal lesions (including the tree-in-bud sign) |
| and/or | | Space-occupying lesions. Lung cavitation and areas of consolidation |
| • the crazy paving sign | | Signs of pulmonary oedema: uniform interlobular septal thickening and pleural effusion |
| Multiple bilateral rounded ground-glass opacities deep in the lung parenchyma: | – | Subpleural reticulation (a mesh pattern) |
| • including those accompanied by consolidation | | Lymphadenopathy without lung lesions |
| and/or | | |
| • the crazy paving sign | | |
| Signs of organising pneumonia: areas of increased density (ground-glass opacities combined with consolidation) and the reversed halo sign | – | |

such abnormalities is now difficult to predict due to little evidence and requires further research. Until these radiographic findings keep improving on follow-up CT scans, they should not be interpreted as “fibrosis” or “sclerosis”, i.e. disease resolution with sequelae. As in community-acquired pneumonia, the duration of resolution of lung abnormalities is not limited and does not correlate with the clinical manifestations of the disease.

The third variant of the evolution of radiographic findings may cause difficulty in differentiating positive and negative changes (Figure 4). If the previous examination was performed before the disease peaked, the time when peak lung involvement is reached, a follow-up image may mislead to a conclusion of disease progression. Clinical manifestations are the key to the interpretation of radiographic findings, which can be accurately assessed only in combination with the clinical picture. If respiratory failure does not become more severe, it indicates regression of the disease, even if the changes in radiographic findings seem to be negative. Radiographic signs have some value too. The signs of OP may be suggestive of disease regression. Worsening of ground-glass opacities, consolidations, reticular changes, and, in many cases, pleural effusion without signs of OP more likely suggests negative evolution.

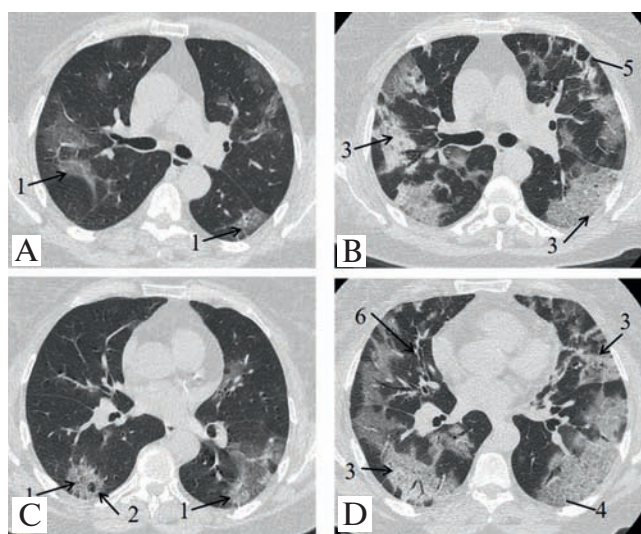


Figure 4. Patient N., 61 years. Moderate COVID-19. Computed tomography, axial slices; A, B, 8th, and C, D, 15th days of the disease. Clinically the patient is stable. A, B, few subpleural inhomogeneous ground glass foci (1) with sporadic secondary lobules with preserved aeration (2). Damaged pulmonary area is about 40%; C, D, multiple confluent areas of increased attenuation (3) predominantly on the periphery; crazy paving symptom (4), peribronchovascular pattern (5), dilated segmental bronchi (6). The lung involvement is about 70%

Рис. 4. Пациентка Н., 61 год. Среднетяжелое течение COVID-19. Компьютерно-томографические аксиальные срезы: А, В – 8-е, С, D – 15-е сутки заболевания. Клинически состояние пациентки стабильное. А, В – немногочисленные субплевральные неомогенные участки «матового стекла» (1) с единичными вторичными дольками с сохраненной воздушностью (2) в их структуре. Площадь поражения легочной паренхимы – около 40%; С, D – множественные сливные фокusy снижения воздушности легочной паренхимы (3), преимущественно в периферических отделах легких; симптом «бульжной мостовой» (crazy paving) (4), уплотнение перилобулярного интерстиция (5), расширенные просветы сегментарных бронхов (6). Площадь поражения легочной паренхимы – около 70 %

Assessment of the extent of lung involvement

From the prognostic point of view, it is important to assess not only the nature of radiographic findings, but also their extent. Assessment of the extent of lung involvement in patients with coronavirus infection can be based on:

- imaging data;
- data obtained using various semiquantitative scales;
- data collected using software for lung density analysis and generation of maps of lung density distribution, including computer-aided design (CAD) and artificial intelligence software solutions.

The literature describes a number of similar scales, developed to improve the early diagnosis of the coronavirus infection and assess its severity more accurately (Tables 4, 5). These scales are almost identical in terms of content and differ only in the total score [36, 40, 42]. It is worth noting that they do not usually consider the type of lung abnormalities (ground-glass opacities and consolidation), except for a 64-point scale developed by *F.Feng et al.* [44]. Their practical application is, however, hindered, because there is an increasing number of publications suggesting the absence of a direct correlation be-

tween the severity of clinical manifestations and the nature and extent of lung injury as assessed by CT [45, 46]. It should also be emphasised that such scoring systems are based on the experience of individual researchers, which leads to some inaccuracy of the results when using them in the general population.

Such semiquantitative assessment of the severity (volume and extent) of CT-diagnosed lung abnormalities associated with COVID-19 is possible, but it is not mandatory. These scales can be used by medical facilities as part of an agreed and approved treatment protocol for COVID-19 patients.

A group of Dutch researchers has proposed an assessment scheme for analysing pulmonary findings in patients with suspected COVID-19, using likelihood ratios (CO-RADS), and presented it on the Radiology Assistant website [47] (Table 6). It was developed as an analogue to previously existing scoring systems (PI-RADS, BI-RADS, etc.), which aim to standardise the assessment of likelihood of a certain diagnosis. Since the CO-RADS is not well known to practitioners and not widely used in inpatient facilities, it has no advantages over semiquantitative scales for assessment of lung abnormalities.

Correlation between imaging findings and infection severity

CT does not assess the severity of the disease and can only provide indirect indicators of its prognosis. Although specialists widely use such terms as “severity of CT findings”, “severity grading of CT findings”, and “severity grades of CT features, such as CT0, CT1, CT2, CT3, CT4, and sometimes CT5”, these data primarily reflect the extent of lung involvement. They poorly correlate with the clinical assessment of the severity of the patient’s condition at the time of CT examination, including such key parameters as the severity of respiratory failure and the degree of desaturation [45, 46].

Multiple publications have reported that patients with severe disease more often have more widespread lung involvement and more frequently develop certain symptoms, for example, reticular changes or pleural effusion. This does not, however, mean that patients with extensive CT or X-ray abnormalities are in critical condition. Importantly, lung lesions can also be found in a considerable number of asymptomatic patients. In the study conducted by *S.Inui et al.*, of 104 cases of coronavirus infection, 76 (73%) were asymptomatic, 41 (54%) of which had pneumonic changes on CT [49]. Our pilot analysis of radiographic and clinical manifestations of 92 patients with COVID-19 showed that two patients (6.9%) with mild infection had extensive lung lesions on a follow CT with > 50% lung involvement, while they did not demonstrate any clinical signs of respiratory failure.

In addition, our own unpublished data demonstrate that bronchodilation on CT obtained at presentation (6.7 ± 2.8 days from onset of the disease) was the only sign that was strongly correlated with the severity

*Table 3
Typical dynamics of pulmonary X-Ray and Computed tomography changes COVID-19 pneumonia [33]*

Таблица 3

Типичные изменения рентгенографической и томографической картины легких в динамике развития пневмонии, обусловленной COVID-19 [33]

| Evolution of changes | Radiographic and CT features | |
|--------------------------------------------|-----------------------------------------------------------------------------------------------------------------------------------------------------------------------------------------------------------------------------------------------------------------------------------------------------------------------------------------------------------------------------------------------------------------------------------------------------------------------------------------------------------------------------------------------------------------------------------------------------------------------------------------------------------------------------------------------------------------------------------------------------------------------------------------------|------------------------------------------------------------------------------------------------------------------------------------------------------------------------------------------------------------------------------------------------------------------------------------------------------------------------------------------------------------------------------------------------------------------------------------------------------------------------------------------------------------------------|
| Early signs observed in the first few days | Multiple bilateral peripheral (subpleural) ground-glass opacities, including those accompanied by consolidation | |
| | and/or | |
| | the crazy paving sign | |
| Improvement of changes (stable disease) | Multiple bilateral rounded ground-glass opacities deep in the lung parenchyma, including those accompanied by consolidation and/or the crazy paving sign | |
| | Areas of increased density (ground-glass opacities combined with consolidation) and the reversed halo sign | |
| | Development of ground-opacities into consolidation (an increase in density of the affected lung tissue) without evident increase in total lung involvement (extent of disease) | |
| Progression of changes (worsening) | Emerging signs of organising pneumonia | |
| | Reduction in size of lung opacities | |
| | Progressive changes (Figure 1): | |
| Respiratory distress syndrome | <ul style="list-style-type: none"> • expansion of ground-glass opacities (extent and volume of lung involvement) • appearance of new ground-glass lesions • fusion of some ground-glass opacities into larger lesions and progression to subtotal lung involvement in the most severe cases • ground-glass opacities are still more extensive than consolidations • Development of new signs of other pathologies: • left ventricular failure (cardiogenic/hydrostatic pulmonary oedema, bilateral pleural effusion) • respiratory distress syndrome (pulmonary oedema) • bacterial pneumonia • lung abscess and multiple septic emboli • pneumothorax and pneumomediastinum • other | |
| | Common features include: | |
| | <ul style="list-style-type: none"> • Bilateral subtotal opacities (consolidations and ground-glass opacities) • Involvement of the upper and middle lung zones • Hyperinflation of basal segments • Gradients in lung density, depending on the patient's position (supine, prone) • The air bronchogram sign | |
| | The following signs are usually absent (in the absence of circulatory failure): | |
| | <ul style="list-style-type: none"> • Kerley lines, peribronchial cuffs • Enlargement of the left heart and increased vascular pedicle width • Pleural effusion | |
| | Resolution | Radiographic signs include: |
| | | <ul style="list-style-type: none"> • Reduction in size of consolidations and ground-glass opacities (the signs of organising pneumonia may not be present) • Appearance of typical CT signs of organising pneumonia and changes in the size and configuration of ground-glass opacities and consolidations |
| | | Additional signs: |
| | | <ul style="list-style-type: none"> • Radiographic signs of resolution should correlate with the evolution of clinical manifestations • Radiographic features of lung damage may persist significantly longer than clinical manifestations of the infection • The presence of residual lung opacities cannot guide the duration of treatment for this infection and do not constitute an indication for continued treatment if not accompanied by clinical signs of acute inflammation |

Table 4
Lung Severity Score scale [42]

Таблица 4
Шкала степени поражения легких [42]

| Degree of lung involvement, % | Score |
|-------------------------------|-------|
| 0 | 0 |
| 1 – 25 | 1 |
| 26 – 50 | 2 |
| 51 – 75 | 3 |
| 76 – 100 | 4 |

Table 5
Chest computed tomography severity score scale [43]

Таблица 5
Шкала тяжести поражения легких по данным компьютерной томографии [43]

| Findings | Score |
|-------------------------------------------------------------------------------------------------------------------|-------|
| Normal attenuation | 0 |
| Ground-glass attenuation | 1 |
| Consolidation | 2 |
| 20 segments (modified classification: 19 lung segments, with one segment being divided into two) | |
| Maximum total score: 40 points (20 × 2) | |
| Interpretation: | |
| The total score of 19.5 or above was predictive of a severe course with a 83.3% sensitivity and a 94% specificity | |

Table 6
CO-RADS scale [47, 48]

Таблица 6
Шкала категориальной схемы компьютерной томографии для пациентов с подозрением на COVID-19 [47, 48]

| CO-RADS score | Level of suspicion of COVID-19 infection | CT findings |
|---------------|------------------------------------------|--------------------------------------------------------------|
| 1 | Very low | Normal or non-infectious abnormalities |
| 2 | Low | Abnormalities consistent with infections other than COVID-19 |
| 3 | Indeterminate | Unclear whether COVID-19 is present |
| 4 | High | Abnormalities suspicious for COVID-19 |
| 5 | Very high | Typical COVID-19 |
| 6 | PCR* | |

of COVID-19 ($p < 0.001$), worsening of clinical status ($p < 0.001$), and an increase in the extent of pulmonary involvement ($p < 0.001$). Other CT findings revealed at initial examination (ground-glass opacity, consolidation, and crazy paving sign) did not show any correlation with the severity of clinical status and had no prognostic value for predicting the worsening of the clinical status. This is indirectly confirmed by some clinical observations of patients with radiographic patterns of similar nature and extent showed different clinical course of COVID-19.

In literature, there is no consensus regarding the prognostic value of separate CT findings. *P.Lyu et al.* showed that the volume of areas with consolidation and the extent of the crazy-paving pattern were significantly greater in severe cases than in mild cases of COVID-19 [50]. The study by *F.Liu et al.* demonstrated the prognostic value of the extent of ground-glass opacities for predicting the worsening of clinical status. The most common sign reported in this study was a combined pattern (any combinations of ground-glass opacities and consolidation) [51].

Correlation between polymerase chain reaction results and chest computed tomography findings

In most studies, CT findings were generally correlated with PCR results [1, 4–6, 52]. There have been, however, some publications reporting positive CT findings despite the negative result of the initial screening PCR test. In the study by *X.Xie et al.* [52], five out of 167 patients with negative initial PCR tests had typical CT features of COVID-19 pneumonia. In all these five patients PRC became positive 2 – 8 days after CT examination. In contrast, seven out of the 167 patients had a normal initial CT, despite a positive initial PCR. Within five days after the initial CT, imaging signs of viral pneumonia were observed in one of these patients, while the follow-up data of the other six patients were not reported. Similarly, *M.Chung et al.* [40] reported that in their study three of 21 patients with a confirmed diagnosis did not have ground-glass opacities or consolidation on their initial CT scans but at the time of re-examination two of them demonstrated positive CT findings. No information was reported about the results of their confirmatory laboratory tests.

H.Kim et al. [53] performed a meta-analysis to evaluate diagnostic values of chest CT and PCR. For chest CT scans, the positive predictive value (PPV) ranged from 1.5 to 30.7%, and the negative predictive value (NPV) ranged from 95.4 to 99.8%. For PCR, the PPV ranged from 47.3 to 96.4%, whereas the NPV ranged from 96.8 to 99.9%. The authors reported that the pooled sensitivity was 94% for chest CT and 89% PCR. The pooled specificity for chest CT was only 37% (95% CI: 26, 50%). The authors suggested that considering a low specificity of CT there is a large gap between PPV levels of chest CT and PCR in low-prevalence regions, especially in areas with a prevalence less than 10%.

These data suggest a high probability of false positive CT findings. This obviously dictates the need for fol-

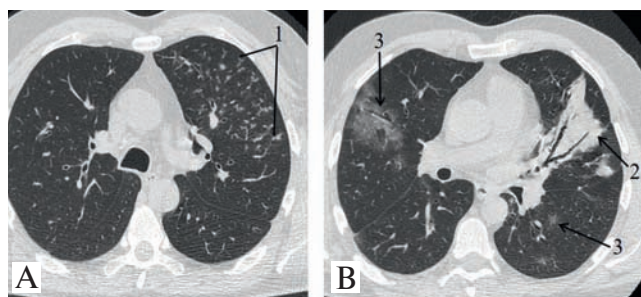


Figure 5. Patient A. 48 years. Moderate COVID-19, complicated by bacterial superinfection. Computed tomography, axial slices, 14th day of the disease. Bronchopneumonia features: tree-in-bud sign (1) in the upper left lobe, segmental consolidation with air bronchogram (2). COVID-19 features: bilateral round-shaped foci of ground glass (3)

Рис. 5. Пациент А., 48 лет. Среднетяжелое течение COVID-19, осложнившееся присоединением бактериальной инфекции. Компьютерная томограмма, аксиальные срезы, 14-е сутки заболевания: признаки бронхопневмонии – симптом «дерево в почках» (1) в верхней доле левого легкого; участок консолидации с воздушной бронхограммой (2). Признаки COVID-19 – билатеральные участки «матового стекла» округлой формы (3)

low-up examinations of people with confirmed disease, resulting in higher healthcare costs and an increasing burden on the healthcare system, as well as growing anxiety on the part of each individual patient and the general population. Moreover, patients with chest CT findings that are only suspicious of COVID-19 could be placed in quarantine, which may cause household problems, difficulties arranging care for children, disabled individuals, or elderly people, or delays in scheduled medical appointments and procedures.

Imaging and etiological diagnosis

Imaging modalities have a high sensitivity for lung involvement in cases suspected for COVID-19. Nevertheless, all of them, including CT, show a low specificity because the same findings can be observed in different lung infections. Certain radiographic findings and their combinations (Table 2) suggest the presence of COVID-19 with a certain probability [33]. The differential diagnosis should primarily include other types of viral pneumonia caused by other coronaviruses (SARS and MERS) and adenoviruses [2, 54, 55].

Pneumonia caused by influenza viruses, adenoviruses, and pneumoviruses (respiratory syncytial virus and human metapneumovirus) may have CT features similar to those of COVID-19. However, they rarely manifest by subpleural lesions. In addition, due to certain pathogenetic factors ground-glass opacities or consolidations can develop in the centrilobular regions [55].

Complications of the novel coronavirus infection (COVID-19)

The following complications of COVID-19 that should be kept in mind while interpreting chest CT findings include: pulmonary embolism (PE), in situ thrombosis of pulmonary vessels, acute heart failure with cardiogenic pulmonary oedema, bacterial superinfection (Figure 5), exacerbation or worsening of chronic lung disease, and treatment complications (pneumothorax, pneumomediastinum, and hematomas) (Figure 6).

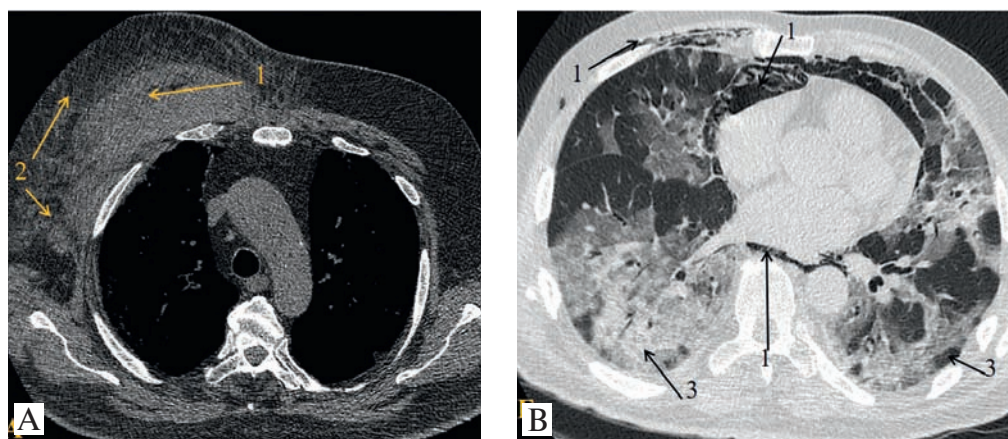


Figure 6. Consequences of the therapy in several patients with severe COVID-19: A, patient T. 74 years, in the intensive care unit department, mechanical ventilation in prone-position. Clinically there is a hematoma at the anterior wall of the right hemithorax. CT, axial slices, 9th day of the disease. Right thoracic muscles are increased in volume (1); stranding and oedema of the anteriolateral subcutaneous fat tissue (2); B, patient K. 74 years, in the intensive care unit department on the mechanical ventilation. CT, axial slices, 2nd day of the disease. Pneumomediastinum (1), subcutaneous emphysema (2). Subtotal increased attenuation of the lung parenchyma (3)

Рис. 6. Последствия проводимой терапии у некоторых пациентов с тяжелым течением COVID-19: А – пациент Т., 74 лет, находится в отделении реанимации и интенсивной терапии, проводится искусственная вентиляция легких в прональной позиции. Объективно у пациента определяется обширная гематома правой половины грудной клетки. Компьютерная томограмма, аксиальный срез, 9-е сутки от начала заболевания: правые грудные мышцы увеличены в объеме (1); подкожно-жировая клетчатка переддверальной поверхности правой половины грудной клетки отечна, тяжиста (2); В – пациент К., 74 лет, находится в отделении реанимации и интенсивной терапии, проводится искусственная вентиляция легких. Компьютерная томограмма, аксиальный срез, 2-е сутки от начала заболевания. Пневмомедиастинум (1), эмфизема мягких тканей (2). Субтотальное уплотнение легочной паренхимы (3) по типу «матового стекла» и консолидации

Pulmonary embolism and in situ thrombosis are associated with endothelial damage, systemic inflammatory reaction, and, as a consequence, hypercoagulation [24, 56]. Suspected PE is an absolute indication for CT angiography. It is, however, rather difficult to suspect thromboembolism in the absence of its typical clinical signs because markers of clot formation are elevated due to COVID-19.

Conclusion

Cardiogenic oedema is another complication of COVID-19. Its manifestation can be associated both with a direct cytotoxic effect of the virus on the myocardium and vascular endothelium and exacerbation of chronic heart failure [57–59]. CT findings include bilateral subtotal consolidations and ground-glass opacities with air bronchogram located in the middle and upper lung zones and intralobular, interlobular, and peribronchovascular interstitial thickening. There are also gradients in lung density, depending on the patient's position (supine, prone) and hyperinflation of basal segments. As circulatory failure progresses, pulmonary abnormalities also become more prominent, patients develop plural effusion (unilateral or bilateral), and enlargement of the left heart becomes visible by imaging modalities [33, 60].

References / Литература

1. Ai T., Yang Z., Hou H. et al. Correlation of chest CT and RT-PCR testing in coronavirus disease 2019 (COVID-19) in China: A report of 1014 cases. *Radiology*. 2020; 296 (2): e32–40. DOI: 10.1148/radiol.2020200642.
2. Franquet T. Imaging of pulmonary viral pneumonia. *Radiology*. 2011; 260 (1): 18–39. DOI: 10.1148/radiol.11092149.
3. Rubin G.D., Ryerson C.J., Haramati L.B. et al. The role of chest imaging in patient management during the COVID-19 pandemic: A multinational consensus statement from the Fleischner Society. *Radiology*. 2020; 296 (1): 172–180. DOI: 10.1148/radiol.2020201365.
4. Nair A., Rodrigues J.C.L., Hare S. et al. A British Society of Thoracic Imaging statement: considerations in designing local imaging diagnostic algorithms for the COVID-19 pandemic. *Clin Radiol*. 2020; 75 (5): 329–334. DOI: 10.1016/j.crad.2020.03.008.
5. Revel M.P., Parkar A.P., Prosch H. et al. COVID-19 patients and the radiology department – advice from the European Society of Radiology (ESR) and the European Society of Thoracic Imaging (ESTI). *Eur. Radiol*. 2020; 30 (9): 4903–4909. DOI: 10.1007/s00330-020-06865-y.
6. Simpson S., Kay F.U., Abbara S. et al. Radiological Society of North America expert consensus statement on reporting chest CT findings related to COVID-19. Endorsed by the Society of Thoracic Radiology, the American College of Radiology, and RSNA – Secondary Publication. *J. Thorac. Imaging*. 2020; 35 (4): 219–227. DOI: 10.1097/RTI.0000000000000524.
7. Soldati G., Smargiassi A., Inchingolo R. et al. Proposal for international standardization of the use of lung ultrasound for patients with COVID-19: A simple, quantitative, reproducible method. *J. Ultrasound Med*. 2020; 39 (7): 1413–1419. DOI: 10.1002/jum.15285.
8. Mit'kov V.V., Safonov D.V., Mit'kova M.D. et al. [RASUDM consensus statement: lung ultrasound in the context of COVID-19 (version 1)]. *Ultrazukovaya i funkcional'naya diagnostika*. 2020; (1): 24–45. DOI: 10.24835/1607-0771-2020-1-24-45 (in Russian). / Митьков В.В., Сафонов Д.В., Митькова М.Д. и др. Консенсусное заявление РАСУДМ об ультразвуковом исследовании легких в условиях COVID-19 (версия 1). *Ультразвуковая и функциональная диагностика*. 2020; (1): 24–45. DOI: 10.24835/1607-0771-2020-1-24-45.
9. Abramowicz J.S., Bassea L.J. [WFUMB Position Statement: how to safely perform ultrasonography and to disinfect ultrasound equipment in the presence of COVID-19]. *Ultrazukovaya i funkcional'naya diagnostika*. 2020; (1): 12–23. DOI: 10.24835/1607-0771-2020-1-12-23 (in Russian). / Абрамович Ю.С., Басси Л.Дж. Заявление о позиции WFUMB: как безопасно проводить ультразвуковое исследование и обеззараживать ультразвуковое оборудование в условиях COVID-19. *Ультразвуковая и функциональная диагностика*. 2020; (1): 12–23. DOI: 10.24835/1607-0771-2020-1-12-23.
10. Piscaglia F., Stefanini F., Cantisani V. et al. Benefits, open questions and challenges of the use of ultrasound in the COVID-19 pandemic era. The views of a panel of worldwide international experts. *Ultraschall Med*. 2020; 41 (3): 228–236. DOI: 10.1055/a-1149-9872.
11. Astuti I., Ysrafil. Severe acute respiratory syndrome coronavirus 2 (SARS-CoV-2): An overview of viral structure and host response. *Diabetes Metab. Syndr*. 2020; 14 (4): 407–412. DOI: 10.1016/j.dsx.2020.04.020.
12. Chan P.K.S., Tang J.W., Hui D.S. SARS: clinical presentation, transmission, pathogenesis and treatment options. *Clin. Sci*. 2006; 110 (2): 193. DOI: 10.1042/CS20050188.
13. Harapan H., Itoh N., Yufika A. et al. Coronavirus disease 2019 (COVID-19): A literature review. *J. Infect. Public Heal*. 2020; 13 (5): 667–673. DOI: 10.1016/j.jiph.2020.03.019.
14. Obadina E.T., Torrealba J.B., Kanne J.P. Acute pulmonary injury: high-resolution CT and histopathological spectrum. *Brit. J. Radiol*. 2013; 86 (1027): 614. DOI: 10.1259/bjr.20120614.

15. Urer H.D., Ersoy G., Yilmazbayhan E.D. Diffuse alveolar damage of the lungs in forensic autopsies: Assessment of histopathological stages and causes of death. *Sci. World J.* 2012; 2012: 657316. DOI: 10.1100/2012/657316.
16. Cardinal-Fernández P., Lorente J.A., Ballén-Barragán A. et al. Acute respiratory distress syndrome and diffuse alveolar damage. new insights on a complex relationship. *Ann. Am. Thorac. Soc.* 2017; 14 (6): 844–850. DOI: 10.1513/AnnalsATS.201609-728PS.
17. Beasley MB. The pathologist's approach to acute lung injury. *Arch. Pathol. Lab. Med.* 2010; 134 (5): 719–727. DOI: 10.1043/1543-2165-134.5.719.
18. Kligerman S.J., Franks T.J., Galvin J.R. From the radiologic pathology archives: Organization and fibrosis as a response to lung injury in diffuse alveolar damage, organizing pneumonia, and acute fibrinous and organizing pneumonia. *RadioGraphics.* 2013; 33 (7): 1951–1975. DOI: 10.1148/rg.337130057.
19. Hansell D.M., Bankier A.A., MacMahon H. et al. Fleischner Society: Glossary of terms for thoracic imaging. *Radiology.* 2008; 246 (3): 697–722. DOI: 10.1148/radiol.2462070712.
20. Leslie K.O. My approach to interstitial lung disease using clinical, radiological and histopathological patterns. *J. Clin. Pathol.* 2009; 62 (5): 387–401. DOI: 10.1136/jcp.2008.059782.
21. Gardenghi G. Pathophysiology of worsening lung function in COVID-19. *Rev. Bras. Fisiol. Exerc.* 2020; 19 (2): S15–S21. DOI: 10.33233/rbfe.v19i2.4058.
22. Mehta P., McAuley D.F., Brown M. et al. COVID-19: consider cytokine storm syndromes and immunosuppression. *Lancet.* 2020; 395 (10229): 1033–1034. DOI: 10.1016/S0140-6736(20)30628-0.
23. Lin L., Lu L., Cao W. et al. Hypothesis for potential pathogenesis of SARS-CoV-2 infection – a review of immune changes in patients with viral pneumonia. *Emerg. Microbes Infectec.* 2020; 9 (1): 727–732. DOI: 10.1080/22221751.2020.1746199.
24. Lorenzo C., Francesca B., Francesco P. et al. Acute pulmonary embolism in COVID-19 related hypercoagulability. *J. Thromb. Thrombolysis.* 2020; 50 (1): 223–326. DOI: 10.1007/s11239-020-02160-1.
25. Baque-Juston M., Pellegrin A., Leroy S. et al. Organizing pneumonia: what is it? A conceptual approach and pictorial review. *Diagn. Interv. Imaging.* 2014; 95 (9): 771–777. DOI: 10.1016/j.diii.2014.01.004.
26. Mehrjardi M.Z., Kahkouee S., Pourabdollah M. Radiopathological correlation of organizing pneumonia (OP): a pictorial review. *Br. J. Radiol.* 2017; 90 (1071): 20160723. DOI: 10.1259/bjr.20160723.
27. Faria I.M., Zanetti G., Barreto M.M. et al. Organizing pneumonia: chest HRCT findings. *J. Bras. Pneumol.* 2015; 41 (3): 231–237. DOI: 10.1590/S1806-3713201500004544.
28. Tisoncik J.R., Korth M.J., Simmons C.P. et al. Into the eye of the cytokine storm. *Microbiol. Mol. Biol. R.* 2012; 76 (1): 16–32. DOI: 10.1128/MMBR.05015-11.
29. Henderson L.A., Canna S.W., Schulert G.S. et al. On the alert for cytokine storm: Immunopathology in COVID-19. *Arthritis Rheumatol.* 2020; 72 (7): 1059–1063. DOI: 10.1002/art.41285.
30. Lomoro P., Verde F., Zerboni F. et al. COVID-19 pneumonia manifestations at the admission on chest ultrasound, radiographs, and CT: single-center study and comprehensive radiologic literature review. *Eur. J. Radiol. Open.* 2020; 7: 100231. DOI: 10.1016/j.ejro.2020.100231.
31. Wynants L., Van Calster B., Collins G.S. et al. Prediction models for diagnosis and prognosis of covid-19 infection: systematic review and critical appraisal. *Br. Med. J.* 2020; 369: m1328. DOI: 10.1136/bmj.m1328.
32. Salehi S., Abedi A., Balakrishnan S., Gholamrezanezhad A. Coronavirus disease 2019 (COVID-19): A systematic review of imaging findings in 919 patients. *Am. J. Roentgenol.* 2020; 215 (1): 87–93. DOI: 10.2214/AJR.20.23034.
33. Sinityn V.E., Tyurin I.E., Mit'kov V.V. [Interim consensus guidelines of the Russian Society of Radiologists and the Russian Association of Ultrasound Diagnostic Specialists in Medicine “Radiological methods for pneumonia diagnosis in new Coronavirus Infection COVID-19”]. *Vestnik rentgenologii i radiologii.* 2020; 101 (2): 72–89. DOI: 10.20862/0042-4676-2020-101-2-72-89 (in Russian). / Синицын В.Е., Тюрин И.Е., Митьков В.В. Временные согласительные методические рекомендации Российского общества рентгенологов и радиологов (РОПР) и Российской ассоциации специалистов ультразвуковой диагностики в медицине (РАСУДМ) «Методы лучевой диагностики пневмонии при новой коронавирусной инфекции COVID-19» (версия 2). *Вестник рентгенологии и радиологии.* 2020; 101 (2): 72–89. DOI: 10.20862/0042-4676-2020-101-2-72-89.
34. Jin Y.H., Cai L., Cheng Z.C. et al. A rapid advice guideline for the diagnosis and treatment of 2019 novel coronavirus (2019-nCoV) infected pneumonia (standard version). *Mil. Med. Res.* 2020; 7 (1): 41. DOI: 10.1186/s40779-020-00270-8.
35. Song F., Zhang X., Zha Y. et al. COVID-19: Recommended sampling sites at different stages of the disease. *J. Med. Virol.* 2020, Apr. 16. DOI: 10.1002/jmv.25892.
36. Pan Y., Guan H., Zhou S. et al. Initial CT findings and temporal changes in patients with the novel coronavirus pneumonia (2019-nCoV): a study of 63 patients in Wuhan,

- China. *Eur. Radiol.* 2020; 30 (6): 3306. DOI: 10.1007/s00330-020-06731-x.
37. Pan F., Ye T., Sun P. et al. Time course of lung changes at chest CT during recovery from coronavirus disease 2019 (COVID-19). *Radiology.* 2020; 295 (3): 715–721. DOI: 10.1148/radiol.2020200370.
 38. Li K., Fang Y., Li W. et al. CT image visual quantitative evaluation and clinical classification of coronavirus disease (COVID-19). *Eur. Radiol.* 2020; 30 (8): 4407–4416. DOI: 10.1007/s00330-020-06817-6.
 39. Hosseiny M., Kooraki S., Gholamrezanezhad A. et al. Radiology perspective of coronavirus disease 2019 (COVID-19): Lessons from severe acute respiratory syndrome and middle east respiratory syndrome. *Am. J. Roentgenol.* 2020; 214 (5): 1078–1082. DOI: 10.2214/AJR.20.22969.
 40. Chung M., Bernheim A., Mei X. et al. CT imaging features of 2019 novel coronavirus (2019-nCoV). *Radiology.* 2020; 295 (1): 202–207. DOI: 10.1148/radiol.2020200230.
 41. Liang T., Liu Z., Wu C.C. et al. Evolution of CT findings in patients with mild COVID-19 pneumonia. *Eur. Radiol.* 2020; 30 (9): 4865–4873. DOI: 10.1007/s00330-020-06823-8.
 42. Bernheim A., Mei X., Huang M. et al. Chest CT findings in coronavirus disease-19 (COVID-19): Relationship to duration of infection. *Radiology.* 2020; 295 (3): 200463. DOI: 10.1148/radiol.2020200463.
 43. Yuan M., Yin W., Tao Z. et al. Association of radiologic findings with mortality of patients infected with 2019 novel coronavirus in Wuhan, China. *PLoS One.* 2020; 15 (3): e0230548. DOI: 10.1371/journal.pone.0230548.
 44. Feng F., Jiang Y., Yuan M. et al. Association of radiologic findings with mortality in patients with avian influenza H7N9 pneumonia. *PLoS One.* 2014; 9 (4): e93885. DOI: 10.1371/journal.pone.0093885.
 45. Zhang B., Zhang J., Chen H. et al. Unmatched clinical presentation and chest CT manifestation in a patient with severe coronavirus disease 2019 (COVID-19). *Quant. Imaging Med. Surg.* 2020; 10 (4): 871–873. DOI: 10.21037/qims.2020.03.12.
 46. Hu X., Hu C.J., Hu J.X. et al. CT imaging of two cases of one family cluster 2019 novel coronavirus (2019-nCoV) pneumonia: inconsistency between clinical symptoms amelioration and imaging sign progression. *Quant. Imaging Med. Surg.* 2020; 10 (2): 508–510. DOI: 10.21037/qims.2020.02.10.
 47. Radiology Assistant. Available at: <https://radiologyassistant.nl> [Accessed: August 07, 2020].
 48. Prokop M., Everdingen W., Rees Vellinga T. et al. CO-RADS: A categorical CT assessment scheme for patients suspected of having COVID-19 – definition and evaluation. *Radiology.* 2020; 296 (2): e97–104. DOI: 10.1148/radiol.2020201473.
 49. Inui S., Fujikawa A., Jitsu M. et al. Chest CT findings in cases from the cruise ship “Diamond Princess” with coronavirus disease 2019 (COVID-19). *Radiol. Cardiothorac. Imaging.* 2020; 2 (2): e200110. DOI: 10.1148/ryct.2020200110.
 50. Lyu P., Liu X., Zhang R. et al. The performance of chest CT in evaluating the clinical severity of COVID-19 pneumonia: Identifying critical cases based on CT characteristics. *Invest. Radiol.* 2020; 55 (7): 412–421. DOI: 10.1097/RLI.0000000000000689.
 51. Liu M., Zhang H., Yu N. et al. Association of CT findings with clinical severity in patients with COVID-19, a multi-center cohort observational study. *Research Square.* [Preprint. Posted: 2020, Apr. 17]. DOI: 10.21203/rs.3.rs-22920/v1.
 52. Xie X., Zhong Z., Zhao W. et al. Chest CT for typical 2019-nCoV pneumonia: Relationship to negative RT-PCR testing. *Radiology.* 2020; 296 (2): e41–45. DOI: 10.1148/radiol.2020200343.
 53. Kim H., Hong H., Yoon S.H. Diagnostic performance of CT and reverse Transcriptase-Polymerase chain reaction for coronavirus disease 2019: A meta-analysis. *Radiology.* 2020; 296 (3): e145–155. DOI: 10.1148/radiol.2020201343.
 54. Koo H.J., Lim S., Choe J. et al. Radiographic and CT features of viral pneumonia. *Radiographics.* 2018; 38 (3): 719–739. DOI: 10.1148/rg.2018170048.
 55. Hani C., Trieu N.H., Saab I. et al. COVID-19 pneumonia: A review of typical CT findings and differential diagnosis. *Diagn. Interv. Imag.* 2020; 101 (5): 263–268. DOI: 10.1016/j.diii.2020.03.014.
 56. Prompetchara E., Ketloy C., Palaga T. Immune responses in COVID-19 and potential vaccines: Lessons learned from SARS and MERS epidemic. *Asian Pac. J. Allergy. Immunol.* 2020; 38 (1): 1–9. DOI: 10.12932/AP-200220-0772.
 57. Fox S.E., Akmatbekov A., Harbert J.L. et al. Pulmonary and cardiac pathology in COVID-19: The first autopsy series from New Orleans. *medRxiv.* [Preprint. Posted: 2020, Apr. 10]. DOI: 10.1101/2020.04.06.20050575.
 58. Long B., Brady W.J., Koyfman A. et al. Cardiovascular complications in COVID-19. *Am. J. Emerg. Med.* 2020; 38 (7): 1504–1507. DOI: 10.1016/j.ajem.2020.04.048.
 59. Ranard L.S., Fried J.A., Abdalla M. et al. Approach to acute cardiovascular complications in COVID-19 infection. *Circ. Heart Fail.* 2020; 13 (7): e007220. DOI: 10.1161/CIRCHEARTFAILURE.120.007220.
 60. Tsuchiya N., Griffin L., Yabuuchi H. et al. Imaging findings of pulmonary edema: Part I. Cardiogenic pulmonary edema and acute respiratory distress syndrome. *Acta Radiol.* 2019; 61 (2): 184–194. DOI: 10.1177/0284185119857433.

Поступила 09.08.20

Received: August 09, 2020

Author Information / Информация об авторах

Igor E. Tyurin – Doctor of Medicine, Professor, Head of the Department of X-Ray and Radiology, Russian Federal Academy of Continued Medical Education, Healthcare Ministry of Russia; tel.: (903) 758-46-52; igortyurin@gmail.com

Тюрин Игорь Евгеньевич – д. м. н., заведующий кафедрой рентгенологии и радиологии Федерального государственного бюджетного образовательного учреждения дополнительного профессионального образования «Российская медицинская академия непрерывного профессионального образования» Министерства здравоохранения Российской Федерации; тел.: (903) 758-46-52; e-mail: igortyurin@gmail.com

Anastasia D. Strutynskaya – Postgraduate student, Russian Federal Academy of Continued Medical Education, Healthcare Ministry of Russia; tel.: (909) 685-75-38; strutynskaya@yandex.ru

Струтынская Анастасия Дмитриевна – аспирант кафедры рентгенологии и радиологии Федерального государственного бюджетного образовательного учреждения дополнительного профессионального образования «Российская медицинская академия непрерывного профессионального образования» Министерства здравоохранения Российской Федерации; тел.: (909) 685-75-38; e-mail: strutynskaya@yandex.ru